FULL PAPER

BJC

British Journal of Cancer (2016) 114, 659–668 | doi: 10.1038/bjc.2016.29

Keywords: prostate tumour; androgen deprivation; bicalutamide; hypoxia; vasculature; IGF-1

Androgen deprivation in LNCaP prostate tumour xenografts induces vascular changes and hypoxic stress, resulting in promotion of epithelial-to-mesenchymal transition

N M Byrne[1,2,4], H Nesbitt[1,4], L Ming[1], S R McKeown[1], J Worthington[3] and D J McKenna*[,1]

[1]*Biomedical Science Research Institute, University of Ulster, Cromore Road, Coleraine, BT52 1SA Northern Ireland, UK;* [2]*Bone Biology Division, Garvan Institute of Medical Research, Darlinghurst, Sydney, NSW 2010, Australia and* [3]*Axis Bioservices Ltd, Research Laboratory, Castleroe Road, Coleraine BT51 3RP, Northern Ireland, UK*

Background: When single-agent androgen deprivation therapy (ADT) is administered for locally advanced prostate cancer, men usually relapse within 1–2 years with more malignant castrate-resistant disease. The reason for this is currently unknown. We now hypothesise that an initial treatment response that increases tumour hypoxia drives selection of more malignant tumours.

Methods: The LNCaP prostate tumour xenografts were analysed for physiological (oxygen and vasculature) and genetic (PCR array) changes during longitudinal treatment with ADT (bicalutamide, 6 or 2 mg kg^{-1} daily for 28 days).

Results: Bicalutamide caused an immediate (within 24 h) dose-dependent fall in oxygenation in LNCaP-luc prostate tumours with a nadir of $\leq$0.1% oxygen within 3–7 days; this was attributed to a significant loss of tumour microvessels (window chamber study). The hypoxic nadir persisted for 10–14 days. During the next 7 days, tumours regrew, oxygenation improved and the vasculature recovered; this was inhibited by the VEGF inhibitor B20.4.1.1. Gene expression over 28 days showed marked fluctuations consistent with the physiological changes. Accompanying the angiogenic burst (day 21) was a particularly striking increase in expression of genes associated with epithelial-to-mesenchymal transition (EMT). In particular, insulin-like growth factor 1 (IGF-1) showed increases in mRNA and protein expression.

Conclusions: Hypoxic stress caused by ADT promotes EMT, providing a mechanism for the cause of malignant progression in prostate cancer.

Androgen deprivation therapy (ADT) is widely used to treat men with advanced localised prostate cancer (PCa). One of the drugs most frequently used for ADT is bicalutamide that slows tumour cell growth through blockade of the androgen receptor (AR). Although initially effective, relapse often occurs within 1–2 years to castrate-resistant prostate cancer (CRPC) that is much more difficult to treat and is often fatal (Hellerstedt and Pienta, 2003). The underlying cause of this tumour progression remains poorly understood.

Hypoxia is a common feature of the tumour microenvironment and hypoxic stress has been linked to changes in a large number of genes (Taiakina *et al*, 2014; Fraga *et al*, 2015). In men, prostate tumours have very low median oxygen levels ($\sim$0.8%; 6.1 mm Hg) compared with the normal tissue ($\sim$4%; 30.5 mm Hg) (McKeown, 2014). It has also been proposed that hypoxia may be the driver of malignant progression in PCa (Rudolfsson and Bergh, 2009).

Previously, we have developed a luciferase-expressing variant of LNCaP prostate cancer cells (LNCaP-luc) that has similar

*Correspondence: Dr Declan J McKenna; E-mail: dj.mckenna@ulster.ac.uk
[4]These authors contributed equally to this work.

Revised 4 January 2016; accepted 14 January 2016; published online 8 March 2016

characteristics to the parental cell line. Although LNCaP cells contain a mutation in the AR, they are androgen sensitive and are widely used as a model for studying androgen sensitivity in prostate tumour xenografts. Initial studies showed that bicalutamide caused an immediate and profound fall in tumour oxygenation that persisted for >10 days; this was followed by a reoxygenation phase, with levels recovering to near pretreatment values within 2 weeks (Ming *et al*, 2013). We have now investigated this effect using a higher dose of bicalutamide (6 mg kg^{-1} daily), consistent with the more widely used clinical dose (150 mg daily). We also investigated the effect of VEGF inhibition on the revascularisation phase. The biphasic response to bicalutamide provided an ideal model for identifying molecular changes accompanying the treatment-induced fluctuations in the tumour microenvironment. In particular, we identified important changes in expression of insulin-like growth factor 1 (IGF-1) and other genes implicated in epithelial-to-mesenchymal transition (EMT); the significance of these genes were further investigated *in vitro*.

MATERIALS AND METHODS

***In vitro* studies.** Androgen-sensitive human LNCaP prostate adenocarcinoma cells were obtained from ATCC (Rockville, MD, USA). A luciferase-expressing variant was developed and confirmed to have similar characteristics to the parental LNCaP cells (Ming *et al,* 2013). Two LNCaP variant cell lines were established from tumours grown in mice and excised after exposure for 28 days to treatment with vehicle (LNCaP-V1) or bicalutamide (LNCaP-B1) (Ming *et al,* 2013). Cells were grown in RPMI-1640 medium (Invitrogen, Paisley, UK) with 10% fetal bovine serum, D-glucose (10 mM) and HEPES (10 mM) and incubated at 37 °C in 5% CO_2 in air. When hypoxic conditions were required, cells were transferred for 4 or 24 h to 0.1% oxygen, 5% CO_2 and 94.9% nitrogen and 37 °C, maintained in an Invivo2 Hypoxia Workstation (Ruskinn Technology, Bridgend, UK). Bicalutamide (Santa Cruz Biotechnology, Heidelberg, Germany) was diluted in 0.01% DMSO. Cells were incubated in vehicle or bicalutamide (4.6 μM) for the times indicated.

***In vivo* studies.** Experiments were conducted in accordance with the Animal (Scientific Procedures) Act 1986 and the UKCCCR guidelines (Workman *et al,* 2010). BALB/c immune-compromised (SCID) mice (8–10 weeks) were housed under standard pathogen-free conditions. During surgery, using aseptic conditions, body temperature was maintained using heated pads. Tumours were established on the backs of SCID mice by subcutaneous injection of LNCaP-luc cells (2×10^6 suspended in 100 μl of matrigel) using a 21-gauge needle. Tumour volume was measured using Vernier calipers (Ming *et al*, 2013). Bicalutamide was prepared in vehicle (0.1% DMSO in corn oil) and administered orally (p.o.) as 2 or 6 mg kg^{-1} daily. The mouse-specific VEGF inhibitor B20-4.1.1 (a gift from Genentech, Inc., San Francisco, CA, USA) was prepared in phosphate-buffered saline and administered intraperitoneally (5 mg kg^{-1}) on days 14 and 17 with daily bicalutamide or vehicle.

Intratumour pO_2 was measured using an OxyLite 2000E system (Oxford Optronix, Oxford, UK) as previously described (Ming *et al,* 2013). The probe was retracted slightly (<5 mm) and left to stabilise for 10 min. Readings were recorded every 10 s for 10 min at two different sites and averaged.

Dorsal skin fold (DSF) preparations were carried out as previously described (Ming *et al,* 2013). Briefly, a bespoke 'window' chamber was attached to the dorsum of mice. A LNCaP-luc tumour fragment was placed in the window, hydrated with sterile saline, covered with a glass coverslip and secured. After 1 week, to allow tumour vascularisation, bicalutamide or vehicle treatment was initiated (day 0). At 5 min before imaging (days 0, 7, 14 and 21), 50 μl of 150 kDa fluorescein isothiocyanate-labelled dextran (FITC-dextran; 50 mg ml^{-1} in saline, Sigma, Poole, UK) was injected into the tail vein. Mice were secured in a bespoke restraint and placed laterally onto a modified microscope stage. Tumour microvessels were imaged using a confocal microscope (Leica Microsystems, Solmes, Germany). Three randomly assigned regions of interest (ROIs) were identified at various locations within each tumour and consecutive images were taken. At each ROI image stacks were created through the *z*-plane with a final maximum projection created using Leica software (LAS AF, Solmes, Germany). Images were analysed offline using ImageJ software (National Institute of Mental Health, Bethesda, MD, USA). Image analysis was performed using stereological 'petrimetrics' techniques (for calculations see Supplementary Information) (Howard and Reed, 2005).

Gene expression analysis. Mice treated daily with vehicle or bicalutamide (2 mg kg^{-1}) were culled on 0, 7, 14, 21 and 28 days post treatment initiation. Tumours were excised and total RNA extracted using Trizol reagent (Invitrogen). Then, 5 μg of RNA per tumour was reverse transcribed using RevertAid (Fermentas, Cambridge, UK) and the cDNA from five tumours per treatment was pooled. RealTime Ready custom 96-well panels (Roche, Sussex, UK) were used to analyse 88 genes selected for their involvement in tumour growth and malignant progression (see Supplementary Information). Plates were prepared and analysed in accordance with the manufacturer's guidelines. Results were normalised to two reference genes (HPRT and β-actin). Fold changes in gene expression of vehicle and bicalutamide-treated xenografts were compared with pretreatment (day 0) expression levels; genes considered upregulated ($\geqslant 2$) or downregulated ($\leqslant 0.5$) that satisfied a *P*-value of <0.05 were deemed statistically significant (Student's *t*-test). Results shown are mean ± s.e. of $\geqslant 5$ pooled tumours analysed in duplicate. Selected genes were also analysed using real-time quantitative PCR (qPCR) (LightCycler 480, Roche). For conditions and primer sequences see Supplementary Information.

Immunohistochemistry (IHC). Excised tumours, treated as indicated, were stained with IGF-1 antibody (1 : 125; Abcam, Cambridge, UK) and detected using IHC Detection Kit (Invitrogen) (further details in Supplementary Information). Scoring was carried out on 5 fields of view at least 20 μm apart (2 sections per slide, two slides per tumour). Staining intensity was scored as negative (0), light (+; 1), medium (++; 2) or dark (+++; 3). Staining extent (i.e., the percentage of cells with cytoplasmic immunoreactivity) was scored as: negative (0), $\leqslant$10% (1), 11–25% (2), 26–50% (3), 51–75% (4) and $\geqslant$76% (5). Extent and intensity scores were added together to provide a score range of 0–8 (Braconi *et al*, 2008). Scores were averaged for three tumours per treatment group.

Statistical analysis. Statistical analysis was carried out using Prism 5.0 software (GraphPad Software Inc., La Jolla, CA, USA). Data from qPCR and tumour growth delay studies were analysed using the two-tailed Student's *t*-test. All differences between points were deemed statistically significant with a $P<0.05$ (95% confidence interval).

RESULTS

Comparison of the effect of 2 and 6 mg kg^{-1} daily bicalutamide on LNCaP tumour growth, oxygenation and metastasis to the lung. Patients are routinely treated daily with either 50 or 150 mg m^{-2} bicalutamide, comparable to 2 and 6 mg kg^{-1} in mice. Daily treatment of LNCaP-luc tumours showed bicalutamide

(both doses) slowed tumour growth, although the effect was small (Figure 1A). However, immediately on initiation of treatment there was a marked effect on tumour oxygenation and by 24 h the oxygen levels had dropped from a starting value of 6 mm Hg (0.8% oxygen) to 1.5 mm Hg (0.2% oxygen) in tumours exposed to 6 mg kg^{-1} bicalutamide. A similar effect was found with 2 mg kg^{-1} bicalutamide; although this dose took somewhat longer to establish a nadir, it was reduced by more than half at 24 h. For both doses the nadir remained until day 14, and this was followed in the next 7 days by a marked increase in oxygenation that was greater for the 6 mg kg^{-1} dose group. By day 28, oxygen levels in the 6 mg kg^{-1} group were equivalent to those in vehicle-treated mice, whereas in the 2 mg kg^{-1} group, although continuing to rise, were slightly lower than vehicle (Figure 1B). Analysis of the excised lungs at day 28 showed metastatic spread in all groups; the increase in metastatic cells in the lungs in the 2 mg kg^{-1} bicalutamide group, although higher than vehicle, was not significant, but the 6 mg kg^{-1} group showed a significant increase ($P<0.05$) (Figure 1C and Supplementary Figure 1).

Bicalutamide caused vascular remodelling in LNCaP tumours commensurate with oxygen changes; anti-VEGF antibody B20.4.1.1 blocked revascularisation. The LNCaP-luc tumours were grown for 7 days in window chambers to allow the vasculature to establish. The mice were then treated with vehicle or bicalutamide (2 or 6 mg kg^{-1}). Representative images show the tumours were well vascularised before treatment (day 0), and no significant change occurred during 21 days of vehicle treatment (Figure 2). However, both 2 and 6 mg kg^{-1} bicalutamide caused a marked fall in microvessel density (MVD) by day 7 that was still evident at day 14. By day 21, revascularisation had occurred.

Stereological analysis of the images showed that MVD (Figure 3A) as well as vessel branch points had decreased significantly at days 7 and 14 for both bicalutamide treatments with partial recovery by day 21 (Figure 3B). In the 2 mg kg^{-1} bicalutamide-treated tumours the average vessel length significantly increased (**$P<0.01$) by 1.9-fold (day 7) and 2.3-fold (day 14) before returning to the pretreatment value by day 21. Similar trends were found with 6 mg kg^{-1} bicalutamide. After 7 days, surviving vessels had significantly larger diameters for both 2 and 6 mg kg^{-1} bicalutamide treatment groups; this was further increased by day 14 and then decreased by day 21, although there was evidence of the persistence of larger vessels for both 2 mg kg^{-1} bicalutamide (***$P<0.001$) and 6 mg kg^{-1} bicalutamide (*$P\leqslant0.05$) (Figure 3C). Commensurate with this, there was an ~15% decrease in the area covered by vessels by days 7 and 14 in both dose groups, and by day 21 this had returned to pretreatment levels (Figure 3D).

The mouse-specific anti-angiogenic VEGF inhibitor B20.4.1.1 has a similar mechanism of action to Avastin (Bagri *et al,* 2010). B20-4.1.1 (5 mg kg^{-1}) was given twice (days 14 and 17), causing a reduction in microvessels by day 21 (Figure 2). When this regimen was combined with daily bicalutamide, it blocked the angiogenic burst caused by bicalutamide alone. Stereological analysis confirmed that B20.4.1.1 inhibited angiogenesis and the vascular recovery caused by bicalutamide (Figure 3).

Identification of molecular changes in LNCaP xenografts during treatment with bicalutamide. The initial biphasic response to bicalutamide was analysed using PCR-array of 88 genes, selected for their involvement in angiogenesis and malignant progression (Supplementary Data). Gene expression is represented as fold change compared with day 0 and significance to vehicle-treated tumours was analysed. Genes that were significantly affected locate above and below the two-fold lines and to the left of the vertical line (Figure 4A). At all time points there were marked changes in gene expression, with much more extensive changes occurring after the initiation of the angiogenic burst identified at day 21. To confirm the reliability of our findings we carried out individual qPCR assessment of three selected genes (*TIMP1*, *IGTA2* and *IGF-1*). Comparison of these three genes on days 7 showed good correlation between the PCR array and the qPCR data (Supplementary Figure 2A). The longitudinal changes observed for six genes implicated in EMT are detailed in Figure 4B. Using IHC a marked change in IGF-1 protein expression was found that correlated well with the mRNA changes found with the PCR array (Figure 5).

Further investigation of selected genes *in vitro*. Exposure of LNCaP-luc cells grown *in vitro* to hypoxia (0.1% oxygen) had little effect on the expression of *IGF-1*, *ITGA2* and *TIMP1* after 4 h; however by 24 h, all three genes were markedly increased. Exposure of the cells to bicalutamide also had a marked effect on gene expression; both *IGF-1* and *ITGA2* increased approximately seven-fold after 24 h, although by 168 h expression they had returned to levels closer to the starting values. In contrast, *TIMP1* showed no increase after 24 h but by 168 h it was 4 times greater. Previously,

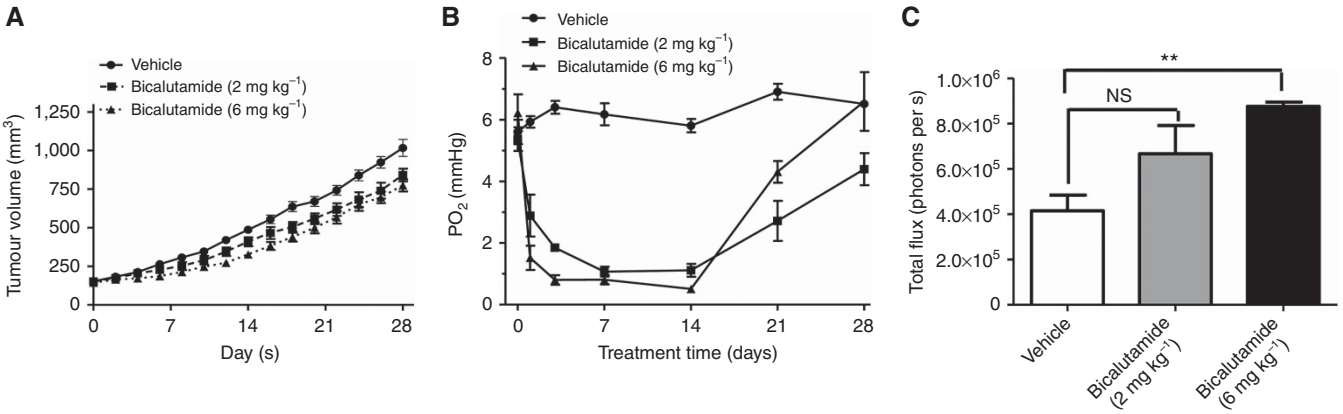

Figure 1. Bicalutamide effect on LNCaP-luc tumour growth, oxygenation and lung metastasis. The SCID mice (8 weeks old) bearing tumours of 100–200 mm^3 were treated daily p.o. for 28 days with vehicle (0.1% DMSO in corn oil) or bicalutamide (2 or 6 mg kg^{-1}). (**A**) Tumour growth. Results: mean ± s.e; $n\geqslant14$ per group. (**B**) Oxygenation during treatment. All data points are significant ($P\leqslant0.001$) except days 0 and 28. (**C**) Quantification of metastasis in lungs of bicalutamide-treated mice compared with vehicle-treated mice. Student's *t*-test *P*-values: NS = not significant, **$P<0.01$.

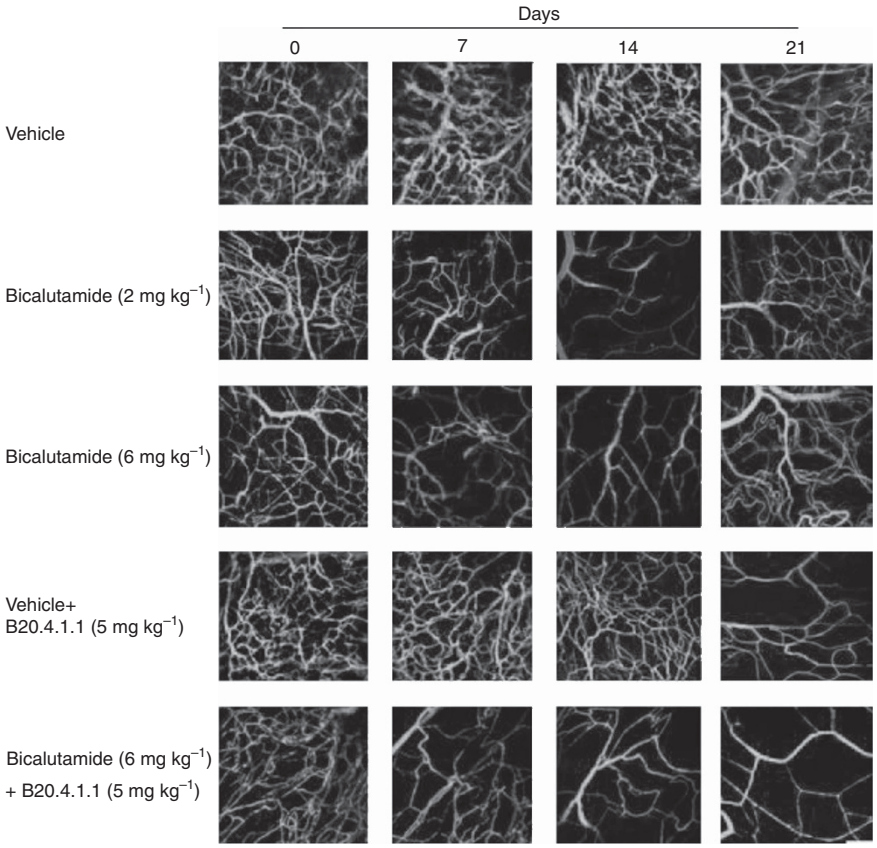

Figure 2. Bicalutamide effect on vascularisation of LNCaP-luc tumour fragments in window chambers. The LNCaP-luc tumour fragments were allowed to vascularise for 7 days. At 15 min before imaging, the vasculature using a confocal microscope FITC-dextran was injected i.v. This was carried out before treatment (day 0) and on days 7, 14 and 21. Treatments: vehicle, bicalutamide 2 or 6 mg kg^{-1} (all p.o.), B20.4.1.1 (5 mg kg^{-1} i.p.) and bicalutamide 6 mg kg^{-1} with B20.4.1.1 administered on day 14. Images ($\times$10 magnification) are representative of $\geqslant$3 mice per treatment. Scale bar = 100 μM.

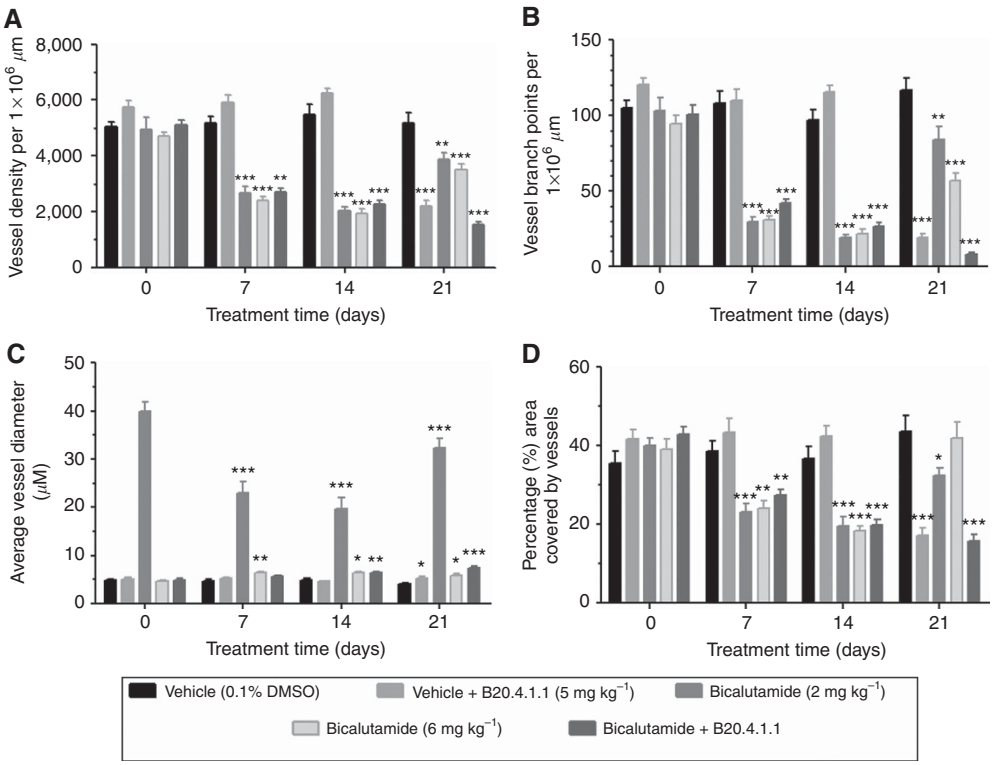

Figure 3. Stereological analysis of window chamber images. Histograms show changes in vessel parameters (**A**) MVD, (**B**) Branch points (**C**) length and (**D**) percentage coverage. Student's *t*-test *P*-values: *$P<0.05$, **$P<0.01$, ***$P<0.001$.

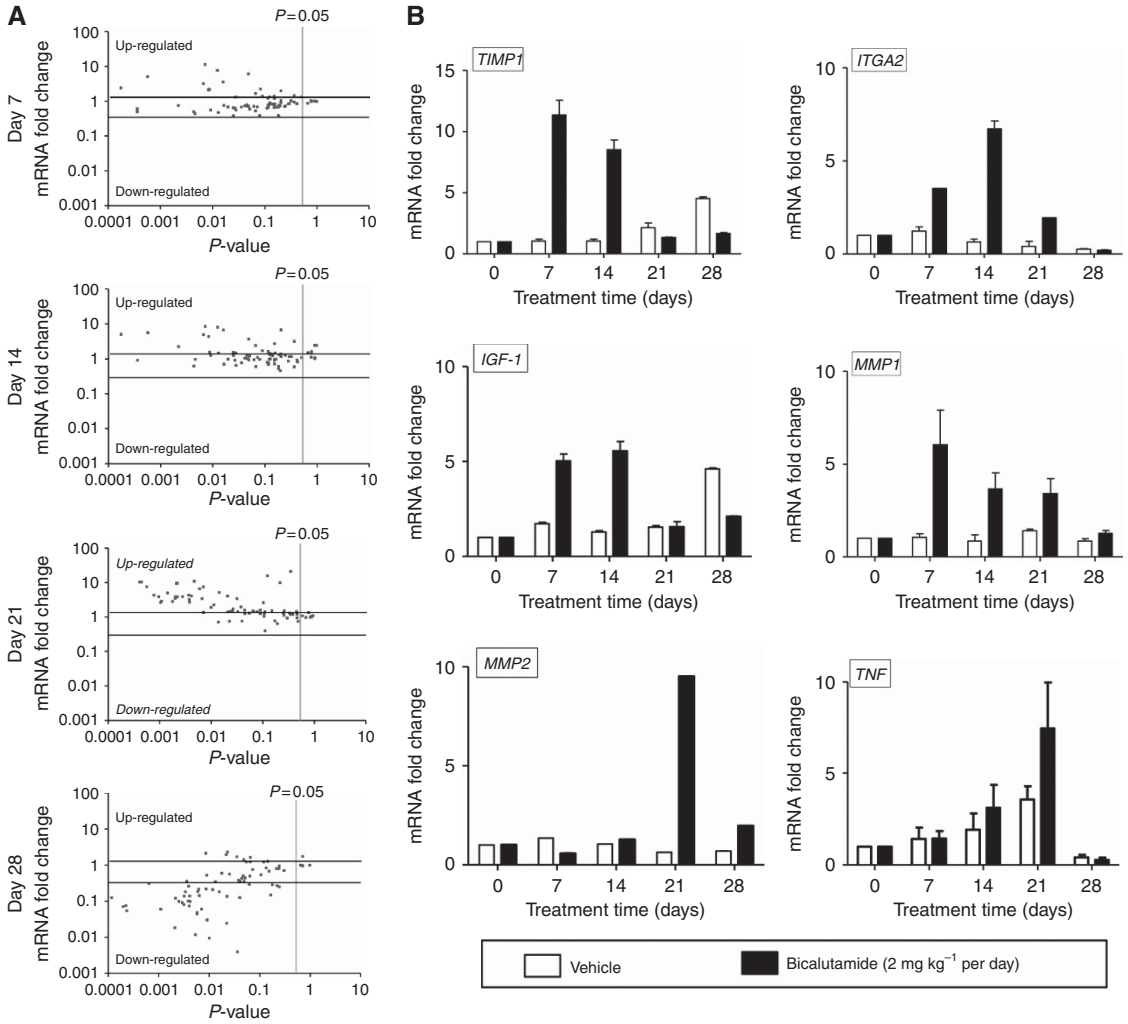

Figure 4. The PCR array analysis of the effect of bicalutamide on LNCaP gene expression. Mice bearing LNCaP-luc tumours (details in Figure 1) were treated daily for up to 28 days with vehicle or bicalutamide (2 mg kg^{-1}). Mice were sacrificed, tumours removed and RNA extracted before treatment (day 0) and at the times indicated. Changes in gene expression were analysed using a PCR array and normalised to two reference genes. Fold changes were compared with day 0. (**A**) Dot plots showing longitudinal gene expression changes. (**B**) Changes in selected genes are detailed, bicalutamide-treated (shaded bars) compared with vehicle-treated controls. Results shown are mean ± s.e. of ⩾5 pooled tumours analysed in duplicate.

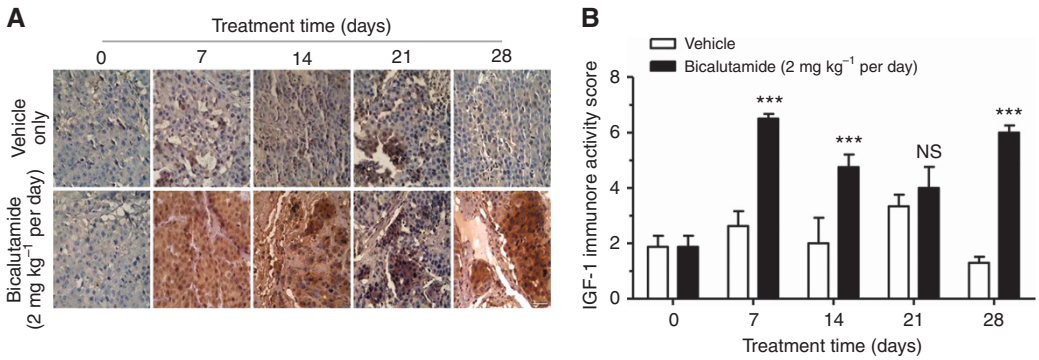

Figure 5. Analysis of IGF-1 protein expression in LNCaP-luc tumours. Tumours were obtained as described in Figure 4, fixed, embedded and stained for IGF-1 immunoreactivity. (**A**) Representative images showing IGF-1 during vehicle or bicalutamide treatment (scale bar = 25 μm) and (**B**) semi-quantification. Results are mean ± s.e. of ⩾3 animals. Student's *t*-test *P*-values: NS = not significant, ***$P<0.001$.

we established two cell lines from LNCaP tumours exposed *in vivo* to vehicle (LNCaP-V1) or bicalutamide (LNCaP-B1) (Ming *et al*, 2013). These cells have higher clonogenic potential and were more resistant to docetaxel (Supplementary Figure 2B–D). Comparison of LNCaP-B1 and LNCaP-V1 showed enhanced levels of Bcl2, VEGF and AR, whereas Bax was decreased (Ming *et al*, 2013).

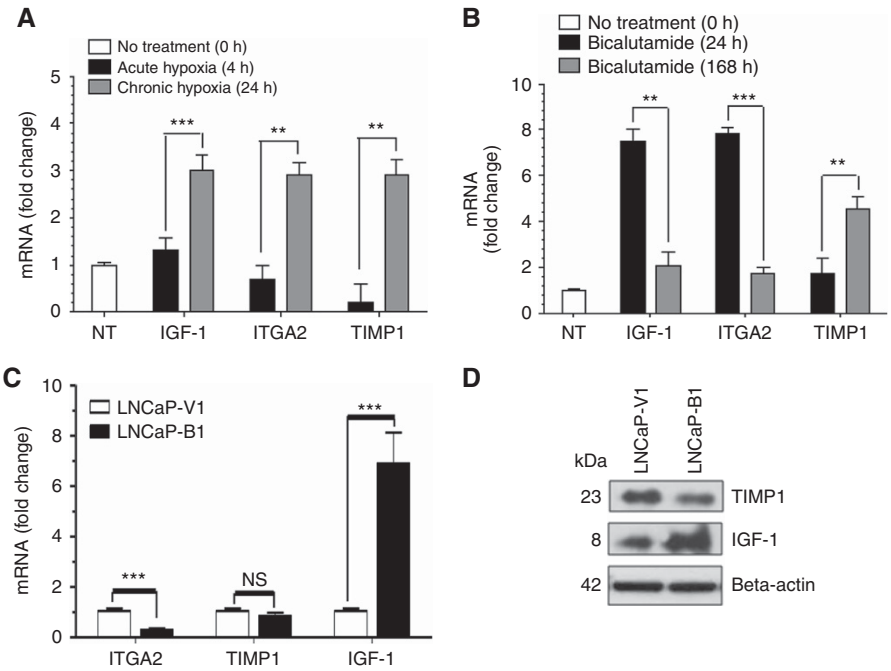

Figure 6. Comparison of the effects of hypoxia and bicalutamide on LNCaP-luc cells. Gene expression of *IGF-1*, *ITGA2* and *TIMP1* was analysed in LNCaP-luc cells grown *in vitro*. (**A**) Cells were exposed to 4 or 24 h hypoxia (0.1%). (**B**) Cells were treated with bicalutamide for 24 or 168 h. (**C**) Gene expression in LNCaP cells isolated from tumours treated *in vivo* with vehicle (V1) or bicalutamide (B1). (**D**) Western blot of IGF-1 and TIMP1 in LNCaP-V1 and LNCaP-B1 cells. Results are mean ± s.e. of 3 independent experiments. Student's *t*-test *P*-values: NS = not significant, $*P<0.05$, $**P<0.01$, $***P<0.001$.

We now show that *ITGA2* is lower in LNCaP-B1 cells, whereas *TIMP1* was unaffected; *IGF-1* was markedly overexpressed, (6.9-fold; $P<0.0001$) (Figure 6C). The IGF-1 protein was also increased in LNCaP-B1 cells (Figure 6D).

DISCUSSION

Progression to CRPC often occurs within 1–2 years of the initiation of ADT, but the primary cause of this relapse is poorly understood. Our study provides direct evidence for an initial prolonged (1–2 week) exposure to severe hypoxia (~0.1% oxygen) caused by androgen deprivation. This slows tumour growth, but it is followed by recurrence of tumours with a more malignant phenotype. Previously, we showed that daily bicalutamide ($2\,mg\,kg^{-1}$) had a marked anti- and then pro-angiogenic effect that explained the biphasic changes in tumour oxygenation (Ming *et al*, 2013). We have confirmed this using a higher dose ($6\,mg\,kg^{-1}$ daily); interestingly, the initial effect was even more immediate and the recovery sharper (Figure 1). Using window chambers we showed significant effects on the tumour vasculature that explained the changes in oxygenation. The changes observed by day 21 might be regarded as 'normalisation' of the vasculature, a feature previously described in a number of models treated with both direct and indirect anti-angiogenic drugs (Fukumura and Jain, 2008). VEGF antibody (B4.20.1.1) over a 7-day period provided the expected anti-angiogenic effect. When combined with daily bicalutamide the angiogenic burst observed with bicalutamide alone was significantly blocked.

Our results are consistent with earlier reports of *in vivo* models. For example, in normal rats castration caused a marked increase in the binding of a hypoxic marker (hypoxyprobe-1) in the prostate, commensurate with the induced vascular collapse (Shabsigh *et al*, 2001). Similarly, castration markedly reduced MVD in normal rat prostate; bicalutamide and finasteride also significantly reduced MVD, although to a lesser extent (Kaya *et al*, 2005). When androgen-dependent Shionogi tumours were grown in nude mice, castration caused a biphasic vascular response, similar to the current study (Jain *et al*, 1998; Hansen-Algenstaedt *et al*, 2000). Hypoxyprobe staining of Myc-CaP prostate tumour xenografts showed hypoxia was present 2 days after surgical castration of the FVB/N mice. This was attributed to tumour blood vessel disruption (CD34+ staining); by day 8, CD34+ cells had reappeared and tumour regrowth followed (Ammirante *et al*, 2014). It may seem counterintuitive that targeting angiogenesis causes a rebound angiogenic burst despite continuing treatment. However, this has been reported in a number of other studies that directly target tumour angiogenesis (Bottsford-Miller *et al*, 2012). The commonality of the hypoxic stress induced by bicalutamide, castration and other antitumour drugs suggests that any treatment that blocks tumour growth is likely, at least in the short term, to inhibit tumour vasculature and as a consequence reduce oxygenation. This may be as a result of a reduction in pro-angiogenic signals from tumour cells that are subjected to androgen deprivation by whatever mechanism. Consequently, it is expected that the newer anti-androgens, for example, enzalutamide and abiraterone, may also initially have similar effects, although the length of these effects may vary and would need further examination.

In human prostate tumours an increase in apoptosis and simultaneous decrease in proliferation markers has been found 1–7 days after castration. Recovery of these markers was found in some patients after 10 days, suggesting that the tumours adapt quite quickly to the new hormone milieu (Ohlson *et al*, 2005). In contrast, in an oxygen electrode study of prostate tumours most patients had no difference (9 out of 22) or an increase (12 out of 22) in oxygen levels in tumours during bicalutamide treatment. However, measurements were only taken before treatment and 30 to 145 days after initiation of daily bicalutamide (150 mg), and it is possible that an initial hypoxic stress was missed (Milosevic *et al*, 2007). Interestingly, our study

suggests that the higher dose of bicalutamide had already reversed the pretreatment oxygen level and it is possible that reoxygenation occurs in most patients treated with bicalutamide monotherapy. In patients treated with daily bicalutamide (50 mg), plus a depot injection of Zoladex (10.8 mg) after 14 days, there was a marked reduction in tumour blood volume and flow, as measured by multiparameter BOLD MRI at 30 days. This effect was sustained for >3 months, confirming that the anti-vascular effect of ADT also occurs in humans (Alonzi *et al,* 2011).

Thus, although these latter two clinical studies gave apparently different results, the main reason for this may be the different treatment regimens used. The study of Alonzi *et al* (2011) is consistent with our findings in LNCaP xenografts that an initial hypoxic stress is caused by bicalutamide. In many patients additional treatments are given such as Zoladex (as Alonzi *et al*, 2011) and/or radiotherapy. The latter is well recognised as a treatment option that can prolong survival of patients treated with ADT (Bria *et al*, 2009). The study of Milosevic *et al* (2007) is consistent with this observed improvement, as adjuvant radiotherapy is usually given between 2 and 4 months after the initiation of ADT and they showed that the oxygenation of many prostate tumours was unchanged or improved after >30 days, although no information on earlier times was provided. It should be noted that for many patients the intratumoural oxygen levels they found (median 5.5 mm Hg, 0.71% oxygen) were still considerably lower than normal prostate tissue (30 mm Hg, 3.9% oxygen) (McKeown, 2014). Our LNCaP xenograft study also shows reoxygenation of the tumours 28 days after bicalutamide continuous monotherapy. At this point we terminated the study because of metastatic spread to the lungs of the mice. In summary, it is proposed that the LNCaP xenograft model is consistent with the published knowledge on tumour responses to ADT. Although the timescales of the effects are somewhat different, it is proposed that the response of LNCaP tumours are sufficiently similar to the human studies to provide a good laboratory model for examining further the genetic changes accompanying ADT, something that would be impossible to model in patients as sequential biopsies are impractical.

Consequently, we have used PCR arrays to identify longitudinal genetic changes caused by ADT in our model. Initially (day 7), the number of genes affected was quite small, indicating inhibition of many tumour responses. In general, they fitted with the expectation of an antitumour effect with a hypoxic response, such as up-regulation of *HIF1A* and *TIMP1* (Figure 4A). During the angiogenic burst (day 21) a large number of genes were significantly upregulated, including several related to EMT. It should also be noted that the vehicle-treated tumours also showed a few, mostly small, changes in gene expression. This is not surprising as the controls were exposed to constant low oxygen levels (~0.8%), a stress that is likely to drive genetic drift, although over a longer time period.

We focussed on results for several genes implicated in angiogenesis and EMT, including *IGF-1*, *ITGA2*, *MMP1*, *MMP2*, *TNF* and *TIMP1* (Figure 4B). The MMPs facilitate tumour cell invasion and metastatic spread whereas TIMPs inhibit MMPs, and consequently the balance of these factors is important in controlling tumour metastasis (Bourboulia and Stetler-Stevenson, 2010). In our study, *TIMP1* was upregulated on days 7 and 14 concomitant to tumour vessel regression and exposure to severe hypoxic (0.1%), consistent with a report that showed *TIMP1* was associated with inhibition of tumour vascularisation in prostate tumour xenografts (Wang *et al*, 2002). As reoxygenation and revascularisation occurred, *TIMP1* expression returned to levels closer to day 0. *MMP1* was elevated on days 7, 14 and 21 and is likely to have had a greater influence on day 21 when *TIMP1* was reduced. At this time, *MMP2* also showed a 10-fold increase. By day 28, the balance between these three genes suggested a switch to a more pro-metastasis genotype than that present on day 0. Previously, bicalutamide was shown to affect a number of genes in LNCaP cells with a shift favouring proteolytic activity (*MMP2*) over their inhibition (*TIMP1*); this was accompanied by a more invasive phenotype (Zhan *et al*, 2002). When MMP1 was overexpressed in LNCaP cells a marked increase in invasion and migration was found and this was paralleled *in vivo* by an increase in tumour growth and lung metastasis; inhibition of MMP1 reversed these effects (Pulukuri and Rao, 2008).

In LNCaP cells either treated with bicalutamide (for 168 h) or exposed to hypoxia (0.1% O_2) for 24 h, we found *TIMP1* significantly increased (Figure 6). However, an elevation in *TIMP1* was not found in the LNCaP-B1 or LNCaP-V1 cells. Some of these variations may reflect cell responses to the *in vitro* environment, especially the 'normal' oxygen levels (20%) used in most studies. The *in vivo* studies mostly support our evidence that *TIMP1* responds early to hypoxic/androgenic stress and is associated, in the longer term, with a more malignant genotype. Other evidence also suggests that initially a raised *TIMP1* may decrease angiogenesis; however, evidence from the literature suggests that in a background of other genetic changes a raised *TIMP1* can be found in more malignant prostate tumours (Daja *et al,* 2003; Oh *et al,* 2011).

We also detected changes in integrin-α2 subunit (*IGTA2*) expression, another gene known to be associated with tumour metastasis. This codes for the α-subunit of the collagen type 1 receptor α2β1 integrin that facilitates adhesion to extracellular matrices. Binding of collagen I to the α2β1 integrin can activate multiple downstream signalling pathways that may facilitate invasion and metastasis and increase the activity of MMPs (Van Slambrouck *et al,* 2009). A recent study has suggested that upregulation of α2β1 integrin in the skeletal metastases of PCa patients may confer a selective advantage for the development of bone metastasis (Sottnik *et al,* 2013). In our study *IGTA2* was significantly upregulated on days 7, 14 and 21, with a >7-fold peak on day 14 (Figure 4). In addition, exposure of LNCaP cells to hypoxia (0.1% O_2) for 24 h upregulated *IGTA2* (Figure 6). Although a definitive link between *IGTA2* expression and hypoxia has yet to be fully elucidated, a previous study reported upregulation of *IGTA2* in diffuse-type gastric cancer cells under hypoxic conditions *in vitro* (1% O_2), mediated via the actions of TGF-β (Noda *et al,* 2010). In a mouse model of breast cancer α2β1 integrin expression was found to inhibit migration, intravasation and anchorage-independent growth *in vitro*. A further analysis of publically available human data in breast and prostate cancer showed that α2β1 integrin was downregulated in more advanced tumours (Ramirez *et al,* 2011). When we exposed LNCaP cells to bicalutamide for 168 h, *IGTA2* was downregulated. In addition, in the LNCaP-B1 cell line, originally isolated after exposure to bicalutamide *in vivo*, *IGTA2* expression was downregulated in comparison with vehicle control cells (LNCaP-V1) (Figure 6). Our evidence suggests that *IGTA2* may be sensitive to tumour microenvironmental changes, and in the longer term downregulation was associated with more malignant disease.

Chronic inflammation is known to promote EMT mediated by a number of factors, including tumour necrosis factor-α (TNFα) and hypoxia (Wu and Zhou, 2009; Balkwill and Mantovani, 2012). In PC3 prostate tumour cells, EMT was induced by prolonged exposure to TNFα through upregulation and stabilisation of the transcriptional repressor Snail (Wang *et al,* 2013). In human and experimental tumours, hypoxia is known to attract accumulation of macrophages that are also known to increase TNFα (Burke *et al,* 2002; Balkwill and Mantovani, 2012). Macrophages can also increase the invasiveness of prostate tumour cells, a process that was blocked by anti-TNFα antibody (Wu *et al,* 2009). In addition, TNFα has been shown to enhance cancer cell invasion by inducing EMT through Snail or ZEB1/ZEB2, both of which are increased

when exposed to IGF-1 (see below). In a recent study of men with advanced PCa treated with ADT it was found that elevated serum levels of both IL8 and TNFα predicted a reduced time to CRPC and overall survival (Sharma *et al,* 2014). In a previous study we showed that bicalutamide-treated tumours showed a marked increase in IL-8. In this study TNFα also increased during treatment, indicating a switch to EMT. A smaller increase in TNFα also occurred in controls, suggesting that, as untreated tumours grow, EMT may also be occurring although at a slower rate.

We were interested to see that *IGF-1* showed marked changes in our study, as it has been linked to EMT in PCa (Li *et al*, 2014). Previously, a meta-analysis of 12 prospective studies found that circulating IGF-1 (but not *IGF-2*) was associated with a moderately increased risk of PCa (Roddam *et al,* 2008). In a comparison of ARPCE (androgen-refractory carcinoma of the prostate, epithelial type) cells to the mesenchymal variant (ARCaPM), a marked elevation of *ZEB1* expression was noted. This protein was also found to be significantly elevated in prostate tumours with a high Gleason score as compared with low-grade tumours and normal tissue. The increase in *ZEB1* was linked to EMT-associated changes, effects that were blocked by ZEB1 siRNA. Importantly, this study showed that the upregulation of *ZEB1* was a downstream consequence of IGF-1 activation of the MEK/ERK pathway (Graham *et al,* 2008).

In early-stage PCa, tumour growth is dependent on AR activation through ligand binding; ADT blocks this process. However, a number of mechanisms can activate the AR independently of ligand binding; these have been associated with progression to CRPC (Katsogiannou *et al,* 2015). A number of growth factors, including IGF-1, were shown to activate the AR in the absence of androgen in prostate tumour cells (Culig *et al,* 1994). In prostate biopsies ($n = 30$) from castrated patients, a drop in IGF-1 expression was found in tumour-derived stromal cells after 7 days, but not in the subsequent 7 days; this was inversely related to the level of apoptosis (Ohlson *et al,* 2005, 2007). These finding are consistent with our study in that there was an immediate anti-proliferative/tumour growth inhibition on initiation of ADT that then resolved to some extent. These authors only measured this up to 14 days, but the data show normalisation of the IGF-1 levels at that time. There is considerable evidence that IGF-1 and AR crosstalk plays an important role in PCa progression and it may also play a pivotal role in controlling metastasis to the bone (Kojima *et al,* 2009). In our study, *IGF-1* was increased approximately four-fold on days 7 and 14. It was still increased on days 21 and 28, although to a moderate extent. We confirmed these finding using IHC to show that the expressed protein levels approximately mirrored the PCR results (Figure 5). Our findings are also consistent with a study of LuCAP35 xenografts in mice that were treated by castration; they showed a significant increase in IGF-1 when excised after 28 days (Sun *et al*, 2012). The results for IGF-1 found in our *in vivo* study were similar to those found *in vitro* (Figure 6). In particular, LNCaP-B1 cells showed a significant increase in IGF-1 expression as compared with LNCaP-V1 control cells. Our study therefore provides evidence that bicalutamide treatment, through its biphasic influence on tumour vasculature/oxygenation, selects for tumours with increased IGF-1 expression that leads to selection for a pro-angiogenic genotype and additional genetic changes linked to EMT.

CONCLUSIONS

Several authors have postulated that the current evidence on the effect of ADT on patients with PCa indicate the need to rethink initial treatment strategies for this patient group (Rudolfsson and Bergh, 2009; Sun *et al*, 2012; Ming *et al,* 2013). Interestingly, a recent study of almost 3000 patients comparing standard of care ADT for $\geqslant 3$ years *vs* ADT with docetaxel for locally advanced PCa has shown that the combination significantly improved survival (James *et al,* 2015), presumably because docetaxel should enhance cell killing at the early stages of ADT, thereby reducing the likelihood of tumour recurrence and increasing survival. Our data show that ADT monotherapy caused a reduction in vascularisation, a profound dose-dependent hypoxia and promoted expression of EMT-associated genes which may help explain why many patients relapse to CPRC within 2 years of starting ADT. We propose that the initial ADT-induced hypoxic stress exerts selection pressure for clones with a more pro-angiogenic, stress-resistant genotype, resulting in the eventual emergence of more malignant tumours. Significantly, this mechanism has also been ascribed to the response of tumours to treatments that directly target tumour angiogenesis (Bottsford-Miller *et al,* 2012). In PCa it occurs in both animal models and men treated with ADT, and thus this mechanism is likely to be a key driver in the development of CRPC. Of particular interest is recent evidence that the targeting of the AR and HIF-1α causes synergistic cell killing, suggesting this approach might provide better control of prostate tumours (Fernandez *et al*, 2015). Previously, we have shown that directly killing hypoxic cells with a hypoxia-activated prodrug (AQ4N) can also have an enhanced antitumour, anti-metastatic effect (Ming *et al*, 2013). This study underlines the importance of recognising that complex physiological and genetic changes occur during ADT for prostate cancer. These studies can inform new strategies for targeting tumours, with an awareness that successful treatment protocols may need to be modified, possibly between treatment cycles, in order to respond to the changing tumour biology.

ACKNOWLEDGEMENTS

This work was supported in part by funding from Prostate Cancer UK and Department of Employment & Learning, Northern Ireland.

CONFLICT OF INTEREST

The authors declare no conflict of interest.

REFERENCES

Alonzi R, Padhani AR, Taylor NJ, Collins DJ, D'Arcy JA, Stirling JJ, Saunders MI, Hoskin PJ (2011) Antivascular effects of neoadjuvant androgen deprivation for prostate cancer: an in vivo human study using susceptibility and relaxivity dynamic MRI. *Int J Radiat Oncol Biol Phys* **80**: 721–727.

Ammirante M, Shalapour S, Kang Y, Jamieson CA, Karin M (2014) Tissue injury and hypoxia promote malignant progression of prostate cancer by inducing CXCL13 expression in tumor myofibroblasts. *Proc Natl Acad Sci USA* **111**: 14776–14781.

Bagri A, Berry L, Gunter B, Singh M, Kasman I, Damico LA, Xiang H, Schmidt M, Fuh G, Hollister B, Rosen O, Plowman GD (2010) Effects of anti-VEGF treatment duration on tumor growth, tumor regrowth, and treatment efficacy. *Clin Cancer Res* **16**: 3887–3900.

Balkwill FR, Mantovani A (2012) Cancer-related inflammation: common themes and therapeutic opportunities. *Semin Cancer Biol* **22**: 33–40.

Bottsford-Miller JN, Coleman RL, Sood AK (2012) Resistance and escape from antiangiogenesis therapy: clinical implications and future strategies *J Clin Oncol* **30**: 4026–4034.

Bourboulia D, Stetler-Stevenson WG (2010) Matrix metalloproteinases (MMPs) and tissue inhibitors of metalloproteinases (TIMPs): Positive and negative regulators in tumor cell adhesion. *Semin Cancer Biol* **20**: 161–168.

Braconi C, Bracci R, Bearzi I, Bianchi F, Sabato S, Mandolesi A, Belvederesi L, Cascinu S, Valeri N, Cellerino R (2008) Insulin-like growth factor (IGF) 1 and 2 help to predict disease outcome in GIST patients. *Ann Oncol* **19**: 1293–1298.

Bria E, Cuppone F, Giannarelli D, Milella M, Ruggeri EM, Sperduti I, Pinnarò P, Terzoli E, Cognetti F, Carlini P (2009) Does hormone treatment added to radiotherapy improve outcome in locally advanced prostate cancer? Meta-analysis of randomized trials. *Cancer* **115**: 3446–3456.

Burke B, Tang N, Corke KP, Tazzyman D, Ameri K, Wells M, Lewis CE (2002) Expression of HIF-1alpha by human macrophages: implications for the use of macrophages in hypoxia-regulated cancer gene therapy. *J Pathol* **196**: 204–212.

Culig Z, Hobisch A, Cronauer MV, Radmayr C, Trapman J, Hittmair A, Bartsch G, Klocker H (1994) Androgen receptor activation in prostatic tumor cell lines by insulin-like growth factor-I, keratinocyte growth factor, and epidermal growth factor. *Cancer Res* **54**: 5474–5478.

Daja MM, Niu X, Zhao Z, Brown JM, Russell PJ (2003) Characterization of expression of matrix metalloproteinases and tissue inhibitors of metalloproteinases in prostate cancer cell lines. *Prostate Cancer Prostatic Dis* **6**: 15–26.

Fernandez EV, Reece KM, Ley AM, Troutman SM, Sissung TM, Price DK, Chau CH, Figg WD (2015) Dual targeting of the androgen receptor and hypoxia-inducible factor 1α pathways synergistically inhibits castration-resistant prostate cancer cells. *Mol Pharmacol* **87**: 1006–1012.

Fraga A, Ribeiro R, Príncipe P, Lopes C, Medeiros R (2015) Hypoxia and prostate cancer aggressiveness: a tale with many endings. *Clin Genitourin Cancer* **13**: 295–301.

Fukumura D, Jain RK (2008) Imaging angiogenesis and the microenvironment. *APMIS* **116**: 695–715.

Graham TR, Zhau HE, Odero-Marah VA, Osunkoya AO, Kimbro KS, Tighiouart M, Liu T, Simons JW, O'Regan RM (2008) Insulin-like growth factor-I-dependent up-regulation of ZEB1 drives epithelial-to-mesenchymal transition in human prostate cancer cells. *Cancer Res* **68**: 2479–2488.

Hansen-Algenstaedt N, Stoll BR, Padera TP, Dolmans DE, Hicklin DJ, Fukumura D, Jain RK (2000) Tumor oxygenation in hormone-dependent tumors during vascular endothelial growth factor receptor-2 blockade, hormone ablation, and chemotherapy. *Cancer Res* **60**: 4556–4560.

Hellerstedt BA, Pienta KJ (2003) The truth is out there: an overall perspective on androgen deprivation. *Urol Oncol* **21**: 272–281.

Howard CV, Reed MG (2005) *Unbiased Stereology. Three Dimensional Measurement in Microscopy*, 2nd edn. Garland Science: New York, NY, USA.

Jain RK, Safabakhsh N, Sckell A, Chen Y, Jiang P, Benjamin L, Yuan F, Keshet E (1998) Endothelial cell death, angiogenesis, and microvascular function after castration in an androgen-dependent tumor: role of vascular endothelial growth factor. *Proc Natl Acad Sci USA* **95**: 10820–10825.

James ND, Sydes MR, Mason MD, Clarke NW, Dearnaley DP, Spears MR, Millman R, Parker C, Ritchie AWS, Russell JM, Staffurth J, Jones RJ, Tolan SP, Wagstaff J, Protheroe A, Srinivasan R, Birtle AJ, O'Sullivan JM, Cathomas R, Parmar MMK (2015) Docetaxel and/or zoledronic acid for hormone-naïve prostate cancer: first overall survival results from STAMPEDE (NCT00268476). *J Clin Oncol* **33**: 2015 (Suppl; abstract 5001).

Katsogiannou M, Ziouziou H, Karaki S, Andrieu C, Henry de Villeneuve M, Rocchi P (2015) The hallmarks of castration-resistant prostate cancers. *Cancer Treat Rev* **41**: 588–597.

Kaya C, Ozyurek M, Turkeri LN (2005) Comparison of microvessel densities in rat prostate tissues treated with finasteride, bicalutamide and surgical castration: a preliminary study. *Int J Urol* **12**: 194–198.

Kojima S, Inahara M, Suzuki H, Ichikawa T, Furuya Y (2009) Implications of insulin-like growth factor-I for prostate cancer therapies. *Int J Urol* **16**: 161–167.

Li P, Yang R, Gao WQ (2014) Contributions of epithelial-mesenchymal transition and cancer stem cells to the development of castration resistance of prostate cancer. *Mol Cancer* **13**: 55.

McKeown SR (2014) Defining normoxia, physoxia and hypoxia in tumours-implications for treatment response. *Br J Radiol* **87**(1035): 20130676.

Milosevic M, Chung P, Parker C, Bristow R, Toi A, Panzarella T, Warde P, Catton C, Menard C, Bayley A, Gospodarowicz M, Hill R (2007) Androgen withdrawal in patients reduces prostate cancer hypoxia: implications for disease progression and radiation response. *Cancer Res* **67**: 6022–6025.

Ming L, Byrne NM, Camac SN, Mitchell CA, Ward C, Waugh DJ, McKeown SR, Worthington J (2013) Androgen deprivation results in time-dependent hypoxia in LNCaP prostate tumours: informed scheduling of the bioreductive drug AQ4N improves treatment response. *Int J Cancer* **132**: 1323–1332.

Noda S, Yashiro M, Nshii T, Hirakawa K (2010) Hypoxia upregulates adhesion ability to peritoneum through a transforming growth factor-beta-dependent mechanism in diffuse-type gastric cancer cells. *Eur J Cancer* **46**: 995–1005.

Oh WK, Vargas R, Jacobus S, Leitzel K, Regan MM, Hamer P, Pierce K, Brown-Shimer S, Carney W, Ali SM, Kantoff PW, Lipton A. (2011) Elevated plasma tissue inhibitor of metalloproteinase-1 levels predict decreased survival in castration-resistant prostate cancer patients. *Cancer* **117**: 517–525.

Ohlson N, Bergh A, Stattin P, Wikström P (2007) Castration-induced epithelial cell death in human prostatetissue is related to locally reduced IGF-1 levels. *Prostate* **67**: 32–40.

Ohlson N, Wikström P, Stattin P, Bergh A (2005) Cell proliferation and apoptosis in prostate tumors and adjacent non-malignant prostate tissue in patients at different time-points after castration treatment. *Prostate* **62**: 307–315.

Pulukuri SM, Rao JS. (2008) Matrix metalloproteinase-1 promotes prostate tumor growth and metastasis. *Int J Oncol* **32**: 757–765.

Ramirez NE, Zhang Z, Madamanchi A, Boyd KL, O'Rear LD, Nashabi A, Li Z, Dupont WD, Zijlstra A, Zutter MM (2011) The $\alpha_2\beta_1$ integrin is a metastasis suppressor in mouse models and human cancer. *J Clin Invest* **121**: 226–237.

Roddam AW, Allen NE, Appleby P, Key TJ, Ferrucci L, Carter HB, Metter EJ, Chen C, Weiss NS, Fitzpatrick A, Hsing AW, Lacey Jr JV, Helzlsouer K, Rinaldi S, Riboli E, Kaaks R, Janssen JA, Wildhagen MF, Schröder FH, Platz EA, Pollak M, Giovannucci E, Schaefer C, Quesenberry Jr CP, Vogelman JH, Severi G, English DR, Giles GG, Stattin P, Hallmans G, Johansson M, Chan JM, Gann P, Oliver SE, Holly JM, Donovan J, Meyer F, Bairati I, Galan P (2008) Insulin-like growth factors, their binding proteins, and prostate cancer risk: analysis of individual patient data from 12 prospective studies. *Ann Intern Med* **149**: 461–471.

Rudolfsson SH, Bergh A (2009) Hypoxia drives prostate tumour progression and impairs the effectiveness of therapy, but can also promote cell death and serve as a therapeutic target. *Expert Opin Ther Targets* **13**: 219–225.

Shabsigh A, Ghafar MA, de la Taille A, Burchardt M, Kaplan SA, Anastasiadis AG, Buttyan R (2001) Biomarker analysis demonstrates a hypoxic environment in the castrated rat ventral prostate gland. *J Cell Biochem* **81**: 437–444.

Sharma J, Gray KP, Harshman LC, Evan C, Nakabayashi M, Fichorova R, Rider J, Mucci L, Kantoff PW, Sweeney CJ (2014) Elevated IL-8, TNF-α, and MCP-1 in men with metastatic prostate cancer starting androgen-deprivation therapy (ADT) are associated with shorter time to castration-resistance and overall survival. *Prostate* **74**: 820–828.

Sottnik JL, Daignault-Newton S, Zhang X, Morrissey C, Hussain MH, Keller ET, Hall CL (2013) Integrin alpha2beta 1 (α2β1) promotes prostate cancer skeletal metastasis. *Clin Exp Metastasis* **30**: 569–578.

SunY Wang BE, Leong KG, Yue P, Li L, Jhunjhunwala S, Chen D, Seo K, Modrusan Z, Gao WQ, Settleman J, Johnson L (2012) Androgen deprivation causes epithelial-mesenchymal transition in the prostate: implications for androgen-deprivation therapy. *Cancer Res* **72**: 527–536.

Taiakina D, Dal Pra A, Bristow RG (2014) Intratumoral hypoxia as the genesis of genetic instability and clinical prognosis in prostate cancer. *Adv Exp Med Biol* **772**: 189–204.

Van Slambrouck S, Jenkins AR, Romero AE, Steelant WF (2009) Reorganization of the integrin alpha2 subunit controls cell adhesion and cancer cell invasion in prostate cancer. *Int J Oncol* **34**: 1717–1726.

Wang H, Fang R, Wang XF, Zhang F, Chen DY, Zhou B, Wang HS, Cai SH, Du J (2013) Stabilization of Snail through AKT/GSK-3β signaling pathway is required for TNF-α-induced epithelial-mesenchymal transition in prostate cancer PC3 cells. *Eur J Pharmacol* **714**: 48–55.

Wang M, Hu Y, Shima I, Stearns ME (2002) IL-10/IL-10 receptor signaling regulates TIMP-1 expression in primary human prostate tumor lines. *Cancer Biol Ther* **1**: 556–563.

Workman P, Aboagye EO, Balkwill F, Balmain A, Bruder G, Chaplin DJ, Double JA, Everitt J, Farningham DA, Glennie MJ, Kelland LR, Robinson V, Stratford IJ, Tozer GM, Watson S, Wedge SR, Eccles SA (2010) Guidelines for the welfare and use of animals in cancer research. *Br J Cancer* **102**: 1555–1577.

Wu Y, Deng J, Rychahou PG, Qiu S, Evers BM, Zhou BP (2009) Stabilization of snail by NF-kappa B is required for inflammation-induced cell migration and invasion. *Cancer Cell* **15**: 416–428.

Wu Y, Zhou BP (2009) Inflammation: a driving force speeds cancer metastasis. *Cell Cycle* **8**: 3267–3273.

Zhan P, Lee EC, Packman K, Tenniswood M (2002) Induction of invasive phenotype by Casodex in hormone-sensitive prostate cancer cells. *J Steroid Biochem Mol Biol* **83**: 101–111.

Supplementary Information accompanies this paper on British Journal of Cancer website (http://www.nature.com/bjc)